THE IMPACT OF AN OROGRAPHIC GRAVITY WAVE DRAG PARAMETERIZATION ON EXTENDED RANGE PREDICTIONS WITH A GCM

W.F. Stern and R.T. Pierrehumbert

Geophysical Fluid Dynamics Laboratory
Princeton, NJ 08542
U.S.A.

1. INTRODUCTION

A major emphasis with regard to the improvement of extended range predictions involves identifying and eventually rectifying those aspects of a GCM's climate that deviate significantly from the observed climate (i.e. model climate drift). Miyakoda et al., (1986) have indicated that most of the error seen in time averaged extended range forecasts is the result of systematic model biases rather than random errors. Inaccuracies in the treatment of convection, cloud-radiation interaction, surface boundary forcing and orography probably account for a significant amount of the systematic errors found in GCMs. Hence, a primary focus for improving atmospheric GCMs, involves development and refinement of parameterizations of those physical processes. One should also not overlook the role of increased resolution in reducing model biases. Higher resolution and improved parameterizations should evolve consistantly, i.e., a parameterization of a subgrid-scale process should ideally converge into an explicit formulation as it becomes a grid-scale process due to increased resolution.

Only recently has the importance of parameterizing subgrid-scale orographic forcing in GCMs been widely recognized. As Miller et al. (1987) have shown, the lack of sufficient drag over continents was not apparent in low resolution models (i.e. R15 and T21 truncations), since it was being compensated by an underestimate in the eddy flux $\langle u'v' \rangle$ which produced reasonable northern hemisphere westerlies, although southern hemisphere westerly flow was too weak. By increasing the resolution (to T40) the bias shifted to the northern hemisphere, as the stronger eddy flux improved the southern hemispheric flow but resulted in over intensification of the northern hemispheric westerlies presumably due to the missing drag. It is in this context that improving the representation of orographic forcing in GCMs has been seen as a mechanism for reducing the northern hemisphere mid-latitude westerly bias. One of the first schemes to successfully address this systematic error involved enhancing a model's mean orography by some multiple of the subgrid-scale orographic variance, i.e., "envelope" mountains (Wallace et al., 1983). More recently, impact studies involving orographic gravity wave drag parameterizations at the Canadian Climate Center (McFarlane 1987) and at the British Meteorological Office (Palmer et al., 1986), have also demonstrated that this westerly bias can be significantly alleviated. These results have motivated efforts to parameterize subgrid-scale orographic forcing in GFDL's Experimental Prediction global spectral model.

In section 2 a description and highlights of the parameterization will be provided. Section 3 describes the experiments and explores the impact of the parameterization on systematic model errors and the main conclusions are summarized in Section 4.

2. PARAMETERIZATION FOR A GCM

Both "envelope" orography and mountain gravity wave drag have been shown to produce similar effects with regard to a model's climate. Yet, they can be thought of as two separate parameterizations: the "envelope" mountains attempt to represent the barrier effect which is missed by the grid-scale mountains and the orographic gravity wave drag scheme simulates the vertical momentum transport by gravity waves generated by flow over subgrid-scale mountains. For this study the focus will be on the parameterization of gravity wave drag due to subgrid-scale orography.

The concepts and theory inspiring this parameterization are detailed by Pierrehumbert (1986), what follows here is primarily an overview. Some key features of this scheme include: a (flow dependent) saturation base momentum flux, acknowledgement of the existence of a low-level regime where strong nonlinear drag enhancement may occur as the result of wave breaking (not included at this stage in the parameterization), and middle and upper atmospheric momentum flux absorption based on a saturation flux profile. The goal is to present a simple parameterization based on fundamental definitions and properties of mountain waves.

2.1 Base Momentum Flux

A key aspect that any parameterization of mountain wave drag must address, is how much

momentum flux is generated at the lower boundary (or mountain top). With the complexities associated with parameterizing a low layer drag, the choice presently is to focus on flux absorption above the surface layer - momentum deposition throughout the depth of the atmosphere should provide a significant impact to the model's general circulation. In this context it suffices to specify the base momentum flux as the residual amount that escapes the low layer region, and treat the nonlinearly enhanced surface drag at a later stage. From 2-D model results, Pierrehumbert (1986) has shown that this residual flux increases linearly for small Fr (<<1) but tends to saturate near the critical point for low layer wave breaking (Fr≈.8), where Fr≡Nh'/U. This leads to a base momentum flux (τ_o) of the following form:

$$\tau_o = -\{\rho U^3/(Nl^*)\}\cdot G \text{ for } N^2>0; =0 \text{ otherwise} \quad (2.1)$$

where,

$$G=G_{max}\ Fr^2/(Fr^2+a^2);\ G_{max},\ a = 1.0 \quad (2.2)$$

N,U are defined as "low-level" (lower 1/3 of model sigma levels) Brunt-Vaisala frequency and wind magnitude, respectively, ρ_o is defined as standard density = 1.13 kg/m^3, l* is an effective mountain length scale, taken as 100 km presently, and h' is subgrid-scale mountain height. The subgrid-scale mountains are obtained from the U.S. Navy 1/6° x 1/6° high resolution topographic dataset. It is interpolated to the GCM's grid to define a mean orography and then the variance (h'^2) is computed for each model grid box. The h' field for a model that uses a 128 x 106 gaussian grid is shown in figure 1. Using N = .01 sec^{-1} and U = 10 m sec^{-1}, those areas exceeding 800 m (shaded) would be getting into the nonlinear regime, for U = 5 m sec^{-1} it would be extended to values of 400 m or more (inside bold contour).

2.2 Momentum Flux Absorption

A second key point which a mountain gravity wave drag must address is how this flux should be distributed in the vertical. In this regard a saturation flux approach has been chosen (see Lindzen, 1981). In general a saturation flux profile, $\tau_s(x,y,p)$, may be defined as a limiting amount of momentum flux above which wave breaking will take place and flux absorption will take place. By applying scale analysis to the definition of wave vertical momentum flux (Pierrehumbert, 1986), the saturation flux profile for waves breaking convectively may be expressed as:

$$\tau_s(p) = -\{\rho_p(p)\cdot U_p^2(p)\cdot D(p)/l^*\cdot G_{max} \quad (2.3)$$

ρ_p and U_p represent vertical profiles of density and wind magnitude and D is a characteristic vertical length of the vertically propagating gravity waves.

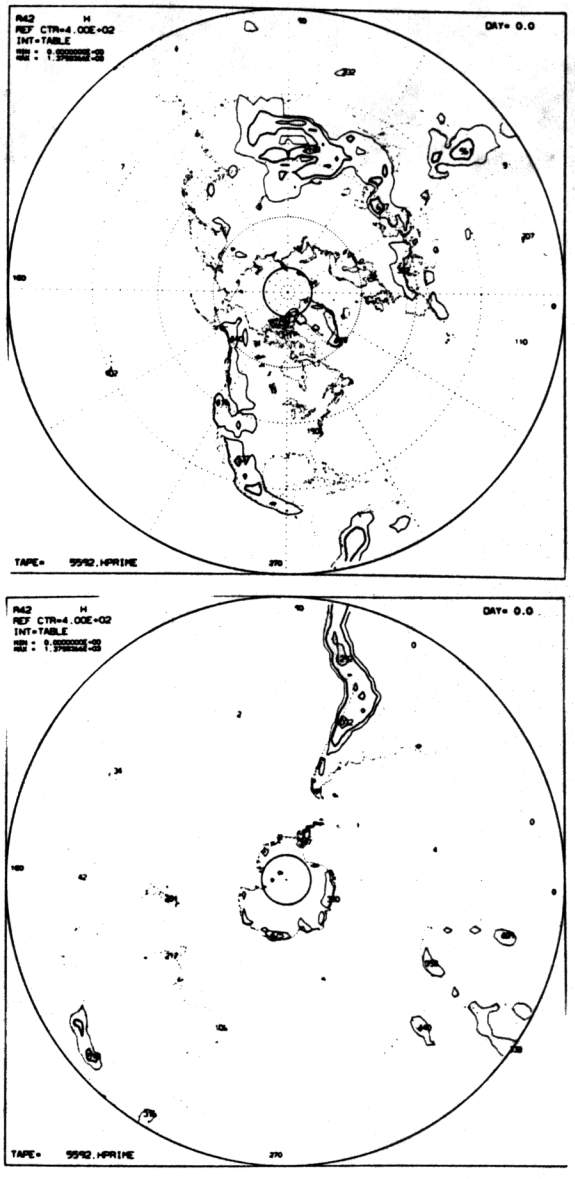

Fig. 1 Subgrid-scale mountains. Lowest contour = 200 m, bold contour = 400 m. Areas > 800 m are shaded. N. hemisphere at top, S. hemisphere at bottom.

In the spirit of establishing a set of baseline sensitivity experiments with which future experiments may be compared, a simple profile which goes to zero linearly in pressure has been adopted, without consideration as to whether any wave breaking criteria has been satisfied. In this case the vertical profile of momentum flux is written as:

$$\tau(p) = (n_x,n_y)\cdot\{1-(p-p_o)/(p_c-p_o)\}\cdot\tau_o \quad (2.4)$$

p_c=0, p_o=surface pressure; n_x=cos(ϕ) and n_y=sin(ϕ) where ϕ=direction of "low level" wind.

A more general vertical profile of τ_s may be determined from 2.3. In order to use this

relation in a parameterization the characteristic vertical length scale of the wave, D, must be calculated. Without any simplifying assumptions it will be a complicated function of height which depends nonlocally on the flow (Pierrehumbert, 1986). By applying the WKB approximation D may be expressed as,

$$D = U_p/N_p \qquad (2.5a)$$

where N_p is the vertical profile of Brunt-Vaisala frequency. However, the use of the WKB approximation is questionable for many atmospheric situations, especially in the vicinity of jet maxima. An extension to the WKB approximation which accounts for curvature in the vertical wind profile should provide for more realistic vertical length scales in regions of strong vertical shear. In this case

$$D^{-2} = \{N_p^2/U_p^2 - \partial^2_z U_p/U_p\} \qquad (2.5b)$$

The actual momentum flux profile will now be determined as follows:

$$\tau_p = \tau_o \text{ at lowest level}$$

$$\tau_p = \tau_{p+1} \text{ (level below) if } |\tau_p| < |\tau_s| \qquad (2.6)$$

otherwise:

$$\tau_p = \tau_s$$

The primary concern is in locating breaking levels in the free atmosphere above a low layer zone where additional wave breaking may be occurring. Hence, the saturation flux profile is fixed to the base flux throughout the low-level region, this prevents the possibility of the parameterization causing breaking to take place in a zone where it is not intended to be valid.

A comparison of zonal mean latitude-height flux absorption profiles is shown in figure 2. The simple linear scheme (2.4) is compared with the wave breaking scheme (using 2.5b with 2.3) for a 9 vertical level model. As expected most of the flux absorption occurs in latitude belts associated with the world's major mountain ranges. Again as one might expect the wave breaking scheme locally produces much larger drag values even though the total is less when integrated vertically and globally. This wave breaking scheme seems to allow considerably more flux absorption in the mid-troposphere and less farther up than some other schemes. The extension to WKB theory given by 2.5b has virtually no effect for either the 9 or 18 level cases. (The location of levels is indicated in figure 3). It seems that the regions where the shear term becomes significant correspond to levels of very strong winds which still inhibit breaking. However, the 18 level profile in addition to being overall more intense than the 9 level, does seem to be indicating more upper tropospheric and lower stratospheric wave breaking, presumably because the relative wind minimum above the jet is better resolved. Also of note is the intense region of flux absorption associated with Antarctica as well as the significant amount associated with Greenland. In this regard, there has been no attempt to treat the subgrid-scale mountains differently whether they are the result of a sharp rise to a plateau or whether they represent a series of ridges and valleys. Furthermore, the subgrid-scale mountains are assumed to have no orientation preference. Clearly both these issues need to be addressed, but for now they are higher order considerations.

3. DESCRIPTION OF EXPERIMENTS AND RESULTS

The model used in this study is a global spectral prediction model including moist convective adjustment, radiative transfer, linear horizontal ∇^4 diffusion, a Monin-Obukhov surface exchange layer and stability dependent vertical turbulent mixing. More details can be found in Gordon and Stern (1982).

Four independent winter initial conditions have been used in this case study. They are 1 January 1977, 1 January 1979, 16 January 1979 and 1 January 1983. Monthly forecasts with (EM) and without (E) orographic

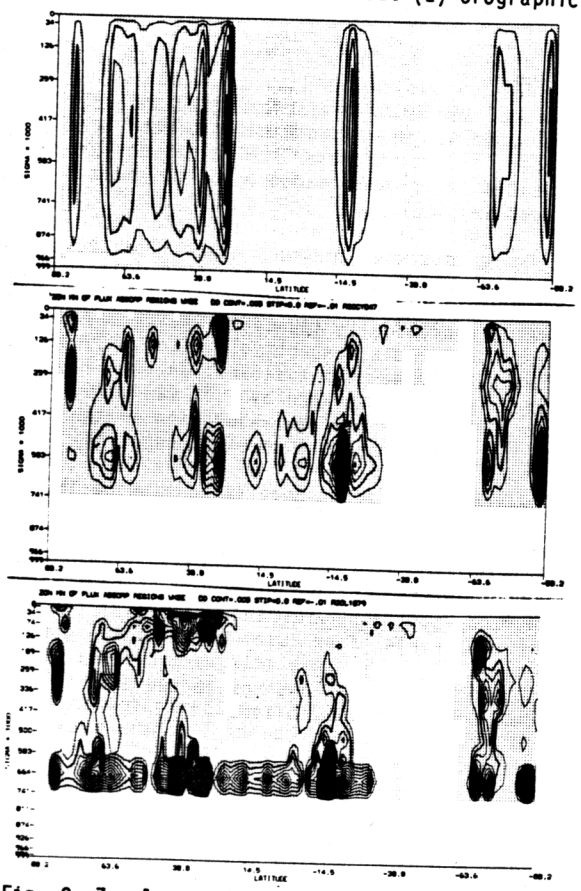

Fig. 2 Zonal mean latitude height flux absorption x-secs based on 1-1-79 initial conditions. Linear scheme for 9 levels at top wave breaking scheme for 9 levels in the middle and wave breaking scheme for 18 levels at bottom.

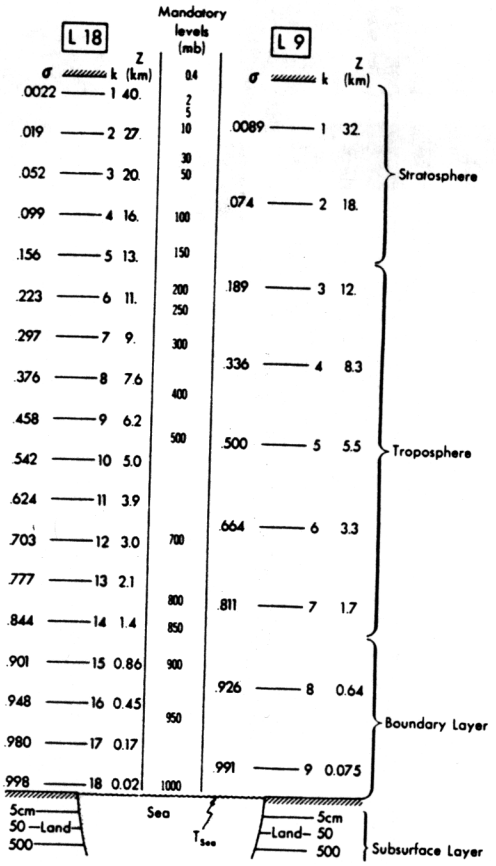

Fig. 3 Vertical levels for 9(L9) and 18(L18) level models. Sigma coordinate values, level indices, and approximate level altitudes are indicated in columns headed by σ, k, and z respectively.

drag were completed for each case. Two sets of predictions were performed with the previously noted spectral model at resolutions of 30 and 42 waves rhomboidally truncated and with 9 and 18 vertical levels respectively (i.e., R30L9 and R42L18). The simple saturation flux vertical profile, defined by 2.4, was used, which allowed for uniform absorption of the base flux throughout the model atmosphere.

The major focus here is to examine the impact of mountain gravity wave drag on the large scale, slowly varying components of the model simulations. In this regard 10, 20 and 30 day time averages have been performed for each forecast. Furthermore, some analyses involve ensemble (four case) means of the time averaged forecasts, this adds more credibility to the results and allows one to see some of the model's systematic biases.

3.1 Westerly Bias

Confirmation of the expected alleviation of the mid-latitude westerly bias may be seen in the R42L18 experiments via figures 4 and 5. Figure 4 presents ensemble mean latitude-height cross sections of the observed zonal mean zonal wind and zonal men zonal wind errors for the forecasts, time averaged over the last 20 days of the forecast period. The most striking difference is the reduction of the westerly wind error in the vicinity of 40°N throughout the troposphere in the mountain gravity wave drag ensemble of cases. The tropical and southern hemisphere model biases have not been reduced, with the easterly bias in the tropical upper troposphere and lower stratosphere even intensifying somewhat. A major improvement at the surface is shown in figure 5. Here the "EM" ensemble mean zonal mean sea-level pressure is significantly closer to the observed than the "E" ensemble, for the northern hemisphere polar latitudes through the mid-latitudes. This is primarily attributed to a "filling" of the Aluetian and Icelandic lows in the cases with mountain drag relative to those without mountain drag. Throughout the tropics and the southern hemisphere there are only small differences between the "E" and "EM" ensemble means, with neither being able to capture the depth of the low pressure belt surrounding the Antarctic continent. Although not shown, similar results have also been obtained from the R30L9 experiments.

3.2 Impact on Forecast Skill

At both resolutions the gravity wave drag parameterization appears to be having a positive impact on the forecasts. RMS 500 mb height errors averaged for the northern hemisphere extratropics and averaged over the 4 cases are shown for R30L9 in figure 6. A significant error reduction for the mountain drag cases is seen for all time averaged forecast results, this reduction is seen at other tropospheric levels as well. Looking at the spectra of the ensemble mean time averaged heights for the forecasts versus observations presents another perspective on systematic model errors. Figure 7 shows northern hemisphere mid-latitude 500 mb height spectra averaged for the last 20 days of the forecasts. This figure reveals that the reduction in RMS height errors for the cases with mountain drag comes mostly from an improved amplitude in zonal wave 0. This is also the case at 1000 mb (not shown). To complete this discussion of forecast skill a synoptic comparison of forecast heights at 500 mb averaged over the last 20 days is presented in figure 8 for the R42L18 forecasts from the 1 January 1983 initial conditions. The most notable improvements for the forecast with mountain drag appear in the ridge-trough system over Europe and to a lesser extent the "fanning" of the height contour over the Rockies and across the U.S.A.

4. CONCLUSIONS

A simple mountain gravity wave drag scheme has been presented which is based on scale analysis concepts applied to fundamental definitions and properties of mountain waves. Using a linear vertical profile of saturation momentum flux, the parameterization was tested in a global spectral model. Generally a positive impact was seen, based on results of monthly forecasts integrated from four initial conditions for two different model resolutions. Specifically, a favorable reduction in the

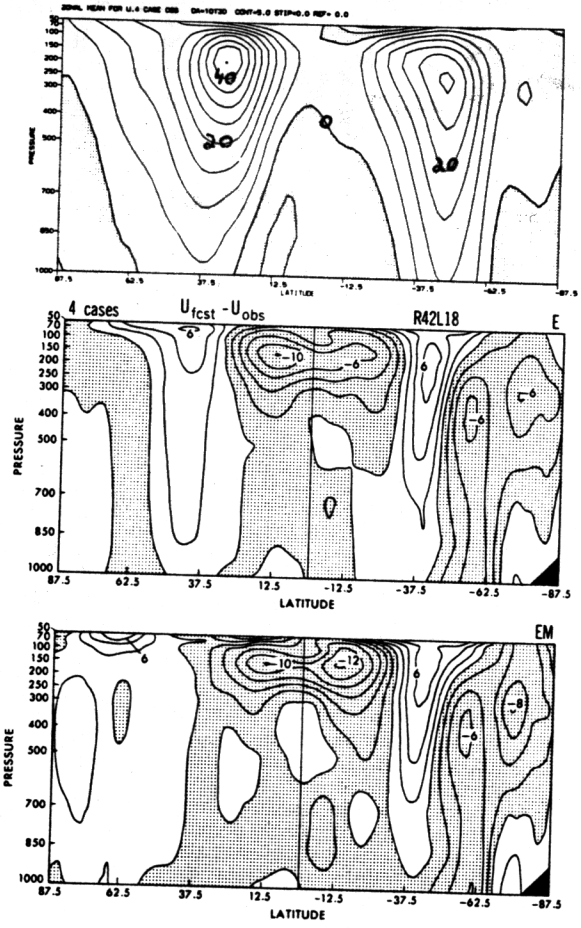

Fig. 4. Latitude-height x-sections of zonal mean zonal wind and zonal wind errors, averaged for the last 20 days of the forecast periods and over the ensemble of 4 cases. Top diagram is the observations and the lower diagrams are the forecast errors for no drag (E) and with drag (EM).

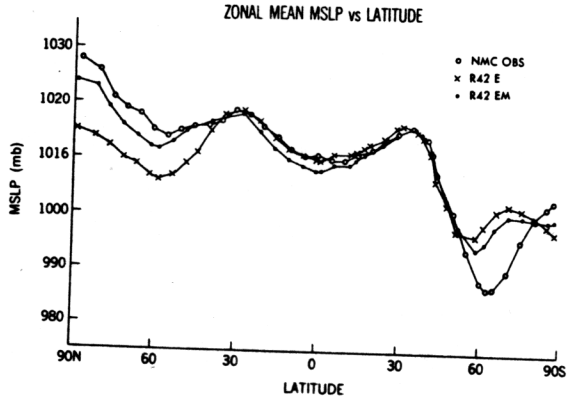

Fig. 5. Monthly mean sea level pressure averaged zonally and averaged over the ensemble of 4 cases.

northern hemisphere mid-latitude westerlies and increased surface pressure, confirms some findings from other models. In addition improved forecast skill has been shown by a reduction in northern hemisphere RMS height errors with most of this improvement in the zonal mean component.

A more complicated vertical momentum flux structure based on the wave breaking flux deposition criteria previously discussed, is currently being tested. Preliminary results indicate that it is performing at least as well as the linear profile.

5. ACKNOWLEDGEMENTS

The authors express their appreciation to Dr. K. Miyakoda for his many helpful suggestions. We are grateful to Mr. Robert Smith for his assistance in producing many of the analyses and thanks to Ms. Wendy Marshall for word processing this manuscript.

6. REFERENCES

Gordon, C.T., and Stern, W.F., 1982: A description of the GFDL global spectral model. Mon. Wea. Rev., 110, 625-644.

Lindzen, R.S., 1981: Turbulence and stress due to gravity wave and tidal breakdown. J. Geophys. Res., 86, 9707-9714.

McFarlane, N.A., 1987: The effect of orographically excited gravity wave drag on the general circulation of the lower stratosphere and troposphere. J. Atmos. Sci., 44, 1775-1800.

Miller, M.J., and Palmer, T.N., 1987: Orographic gravity-wave drag: its parameterization and influence in general circulation and numerical weather prediction models. (Submitted for publication)

Miyakoda, K., Sirutis, J. and Ploshay, J., 1986: One-month forecast experiments - without anomaly boundary forcings. Mon. Wea. Rev., 114, 2363-2401.

Palmer, T.N., Shutts, G.J. and Swinbank, R., 1986: Alleviation of a systematic westerly bias in general circulation and numerical weather prediction models through an orographic gravity wave drag parameterization. Quart. J. R. Met. Soc., 112, 1001-1039.

Pierrehumbert, R.T., 1986: An essay on the parameterization of orographic gravity wave drag. To be published in proceedings from ECMWF 1986 Seminar.

Wallace, J.M., S. Tibaldi and A.J. Simmons, 1983: Reduction of systematic errors in the ECMWF model through the introduction of an envelope orography. Q. J. Roy. Meteor. Soc., 109, 683-717.

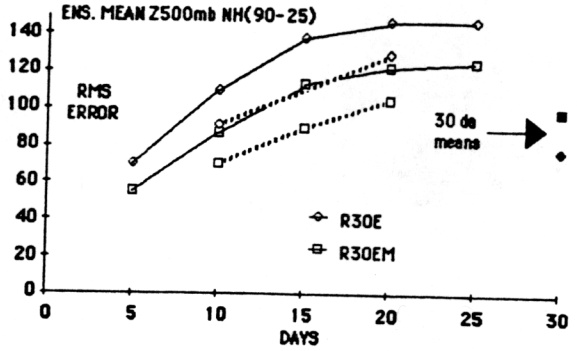

Fig. 6. Ensemble mean (4 case) RMS errors for 500 mb height, with (EM) and without (E) mountain gravity wave drag. Solid lines are for 10 day mean and dashed are for 20 day means.

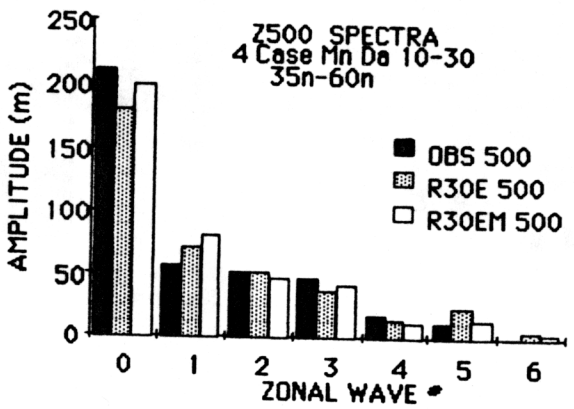

Fig. 7. Ensemble mean 500 mb height field averaged over last 20 days of the forecasts as a function of zonal wave number.

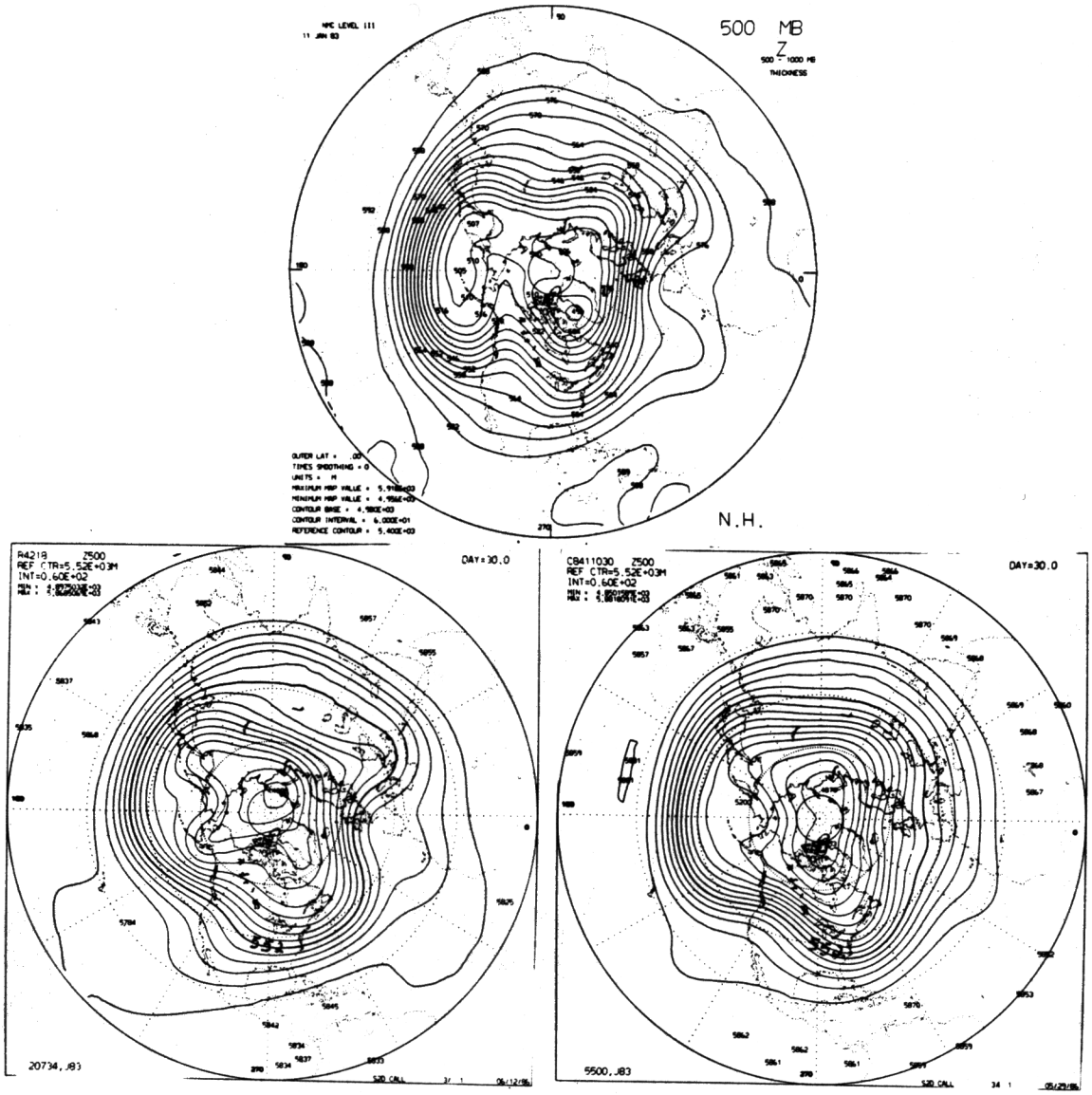

Fig. 8. 500 mb height time averaged from 11 Jan 83 -> 30 Jan 83 for NMC observations (top center), R42L18 with drag (lower left) and R42L18 without drag (lower right).